Fanno processes in dense gases

M. S. Cramer, J. F. Monaco, and B. M. Fabeny

Citation: Physics of Fluids (1994-present) **6**, 674 (1994); doi: 10.1063/1.868307
View online: http://dx.doi.org/10.1063/1.868307
View Table of Contents: http://scitation.aip.org/content/aip/journal/pof2/6/2?ver=pdfcov
Published by the AIP Publishing

Fanno processes in dense gases

M. S. Cramer, J. F. Monaco, and B. M. Fabeny
Engineering Science and Mechanics, Virginia Polytechnic Institute and State University, Blacksburg, Virginia 24061-0219

(Received 9 June 1993; accepted 6 October 1993)

The global behavior of Fanno processes is examined for dense gases. It is shown that three sonic points corresponding to two local maxima and one local minimum in the entropy can occur if the fluid is of the Bethe–Zel'dovich–Thompson type. Both analytical and numerical examples of the nonclassical behavior are provided.

I. INTRODUCTION

One of the simplest models for the frictional heating of gases is the Fanno process. This model takes the flow to be one-dimensional, steady, and adiabatic and is discussed in most texts on gas-dynamics,[1] engineering thermodynamics,[2] and engineering fluid mechanics.[3] Although the most common method of presentation involves the use of perfect gases, many applications of interest involve large pressures. In such high-pressure applications the ideal gas model may no longer give an accurate estimate of the thermodynamic properties and a more complex equation such as that due to van der Waals is required. Examples of high speed flows in which dense gas effects are important include the hypersonic and transonic wind tunnel designs described by Enkenhus and Parazzoli,[4] Simeonides,[5,6] Anderson,[7,8] and Anders;[9] the transport of fuels and other chemicals described by Leung and Epstein,[10] and Bober and Chow;[11] and the cooling of hypersonic aircraft described by Dziedzic *et al.*[12] Heat transfer and turbomachinery equipment in both subcritical and supercritical Rankine power cycles also frequently involve dense gas effects; see, e.g., Jones and Hawkins[2] and Reynolds and Perkins.[13]

The purpose of the present study is to develop a more complete theory of Fanno flows which is valid for the full range of pressures and temperatures encountered by single-phase fluids. We will also expand the scope of the analysis to include the full range of fluids of interest in applications such as chemical and fuel transport, novel wind tunnel designs, and Rankine cycle power systems.

Previous investigations of Fanno flows using more general equations of state are reported by Landau and Lifshitz[14] and Arp *et al.*[15] The former authors presented a series of local results valid for all gas models. The latter authors emphasized the importance of the Grüneisen parameter, $\beta a^2/c_p$, on the flow behavior. Here

$$\beta \equiv -\frac{1}{\rho}\frac{\partial \rho}{\partial T}\bigg|_p \tag{1}$$

is the coefficient of thermal expansivity, c_p is the specific heat at constant pressure and

$$a \equiv \left(\frac{\partial p}{\partial \rho}\bigg|_s\right)^{1/2} \tag{2}$$

is the thermodynamic sound speed. The quantities p, ρ, s, and T are the fluid pressure, density, entropy, and absolute temperature.

Striking qualitative differences between the perfect gas and dense gas theory were first revealed by Thompson,[16] who demonstrated the critical importance of the fundamental derivative

$$\Gamma \equiv \frac{a}{\rho}+\frac{\partial a}{\partial \rho}\bigg|_s = \frac{1}{\rho}\frac{\partial (\rho a)}{\partial \rho}\bigg|_s \tag{3}$$

to virtually all aspects of gas dynamics. With respect to Fanno flows, Thompson's main contribution was to prove that any sonic point in a $\Gamma < 0$ fluid will correspond to a local minimum in the flow entropy. In order that the entropy increase in Fanno flows, all flows would then be driven *away* from the sonic, i.e., choking, condition provided that the $\Gamma < 0$ assumption is satisfied. This contrasts with the well-known perfect gas theory where $\Gamma > 0$ and all flows necessarily become sonic, i.e., choked, provided that the duct length is sufficiently large. Thompson[16] gives a definitive picture of the Fanno process provided the fundamental derivative (3) is either strictly positive or strictly negative. The main goal of the present study is to extend Thompson's analysis to flows for which Γ can change sign within the flow. We also provide specific numerical examples of the nonclassical flows predicted by both Thompson and the present authors.

Because of the central role played by Γ in the following study, we first provide a brief review of its variation and the conditions under which it becomes negative. The first to give a detailed discussion of the variation and sign of (3) were Bethe[17] and Zel'dovich,[18] who demonstrated that Γ can become negative over a finite range of pressures and temperatures in fluids with sufficiently large specific heats. For a given fluid with a large specific heat, the range of pressures and temperatures corresponding to $\Gamma < 0$ is in the general neighborhood of the saturated vapor line at pressures on the general order of the value at the thermodynamic critical point. To provide examples of negative Γ fluids and to illustrate the general variation of Γ we have plotted a scaled version of Γ as a function of scaled density on the critical isotherm in Fig. 1. The fluids chosen are molecular nitrogen (N_2), steam (H_2O), octane (C_8H_{18}), and four commercially available heat transfer fluids: FC-72 (C_6F_{14}), PP9 ($C_{11}F_{20}$), PP11 ($C_{14}F_{24}$), and FC-71 ($C_{18}F_{39}N$). The physical properties for the first three fluids

 1070-6631/94/6(2)/674/10/$6.00

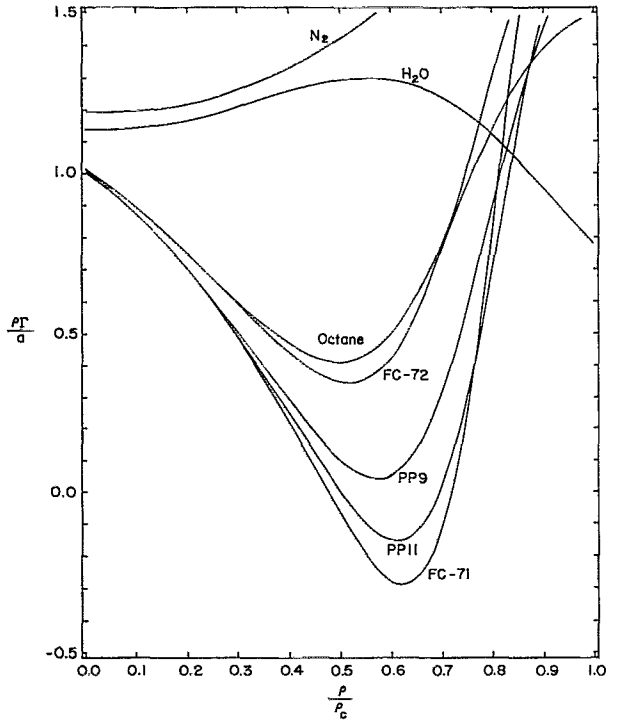

FIG. 1. Variation of the fundamental derivative (3). In each case the temperature is the critical temperature of the fluid of interest.

were taken from Reid *et al.*[19] and those for FC-72 and PP9 were taken from the manufacturer's technical publications. The required physical properties of PP11 and FC-71 were estimated by Cramer.[20] The equation of state employed for the generation of Fig. 1 is that due to Martin and Hou.[21] Full details of the implementation used may be found in the article by Cramer.[20]

The main point to note in Fig. 1 is that the heavier fluids have a local minimum in $\rho\Gamma/a$ at about one-half to two-thirds the critical density. The heaviest fluids, viz., PP11 and FC-71, have a finite region of $\Gamma<0$ at the critical temperature. It should be noted that both Lambrakis and Thompson[22] and Cramer[20] have shown that PP9 also admits a range of pressures and (subcritical) temperatures in its single-phase regime for which $\Gamma<0$, even though the gas model used here yields $\Gamma>0$ at the critical temperature. Further examples of negative Γ fluids are found in the work of Thompson and Lambrakis.[23] Summaries of the nonclassical dynamics possible in such fluids can be found in the articles by Thompson,[16] Thompson and Lambrakis,[23] Menikoff and Plohr,[24] Leidner,[25] and Cramer.[26]

The previous investigations of negative Γ fluids indicate that the variation of $\rho\Gamma/a$ on isotherms, isentropes, shock adiabats, and Fanno lines is qualitatively the same as that plotted in Fig. 1. Because of the importance of fluids having such a negative Γ region and the pioneering work done by the authors mentioned above, we will refer to any fluid which possesses such a $\Gamma<0$ region as a Bethe–Zel'dovich–Thompson (BZT) fluid.

In the next section we lay out the general theory of Fanno flows. Many of the results proven in this section will be similar to those developed by Landau and Lifshitz[14] and Thompson,[16] although the present authors account for the global features of the Fanno curve, including sign changes in Γ. In Secs. III–V, we provide specific examples of nonclassical Fanno flows. In particular, we present analytical solutions for the Fanno curve corresponding to van der Waals gases in Sec. III and numerical solutions using the van der Waals gas model and the more accurate Martin–Hou model in Secs. IV and V. In Sec. VI we provide a short discussion of possible shocked Fanno flows.

II. GENERAL THEORY

The governing equations of a Fanno flow may be derived by taking the flow to be single-phase, one-dimensional, adiabatic, free of body forces, and steadily flowing in a constant area duct. The resultant mass and energy equations may therefore be written[1]

$$v\rho=v/V=\dot{m}=\text{const}, \tag{4}$$

$$h+\dot{m}^2V^2/2=\text{const}. \tag{5}$$

Here v is the particle velocity, $V\equiv\rho^{-1}$ is the specific volume, $\dot{m}$ is the mass flux, and h is the enthalpy

$$h\equiv e+p/\rho, \tag{6}$$

where e is the internal energy. Because the flow is adiabatic and involves fluid friction, we naturally assume that the entropy increases with distance along the duct. As a result, we will impose the following condition as the expression for the second law of thermodynamics:

$$\frac{ds}{dx}>0, \tag{7}$$

where the x axis will be taken as positive in the direction of the flow. In fact, if we consider a general fluid flowing through a duct with a circular cross section of diameter D, the equation expressing conservation of linear momentum may be combined with identities derived later in this section to show that

$$\frac{ds}{dx}=\frac{4\tau_w}{\rho T D}, \tag{8}$$

where $\tau_w=\tau_w(x)$ is the shear stress at the duct wall, defined so that $\tau_w>0$ if the force generated on the fluid opposes the direction of flow. Thus (7) is consistent with the expectation that fluid friction opposes the motion. Furthermore, the use of the strict inequality in (7) is consistent with the expectation that the friction remains nonzero.

Inspection of (5) reveals that the Fanno line is simply a downward facing parabola in the h-V plane. In the subsequent discussion it will also be useful to determine the qualitative features of the isentropes. If we employ Gibbs' relation

$$dh=T\,ds+\frac{1}{\rho}dp, \tag{9}$$

it may be shown that

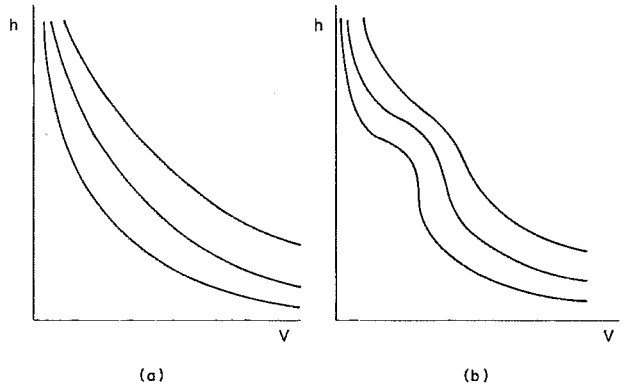

FIG. 2. Sketch of the isentropes in the h-V plane for (a) a fluid having $\rho\Gamma/a>\frac{1}{2}$ everywhere and (b) a fluid having $\rho\Gamma/a<\frac{1}{2}$ over a finite range of V.

$$\left.\frac{\partial h}{\partial V}\right|_s=-\frac{a^2}{V}<0, \tag{10}$$

$$\left.\frac{\partial h}{\partial s}\right|_V=T\left(1+\frac{\beta a^2}{c_p}\right)>0. \tag{11}$$

From (10), it is clear that the slopes of the isentropes in the h-V plane are also negative. Although the thermal expansivity β can be negative for liquids, e.g., pure water between 0 and 4 C, we will take $\beta>0$ for all vapors considered in the present study. The nonclassical effects which arise when $\beta<0$ have been summarized in Sec. V of Menikoff and Plohr.[24] The inequality in (11) is an immediate consequence of the $\beta>0$ assumption once the well-known constraint $(c_p>c_v>0)$ is imposed; here c_v is the specific heat at constant volume. We conclude that the isentropes do not intersect and that the isentropes corresponding to the largest entropies lie above those having lower entropies in the h-V plane. Although it is clear that the Fanno line is always concave down, the isentropes may or may not be strictly concave up. The precise condition may be seen by inspection of the following second derivative:

$$\left.\frac{\partial^2 h}{\partial V^2}\right|_s=\frac{a^2}{V^2}\left(2\frac{\rho\Gamma}{a}-1\right). \tag{12}$$

Thus the isentropes are concave up in the h-V plane whenever $\rho\Gamma/a>1/2$ and concave down whenever $\rho\Gamma/a<1/2$. Similar conclusions have also been given by Thompson.[1,16] Isentropes corresponding to a fluid having $\rho\Gamma/a>1/2$ everywhere and a fluid having $\rho\Gamma/a<1/2$ over a finite range of volumes are sketched in Fig. 2.

The entropy variation along a Fanno line can be deduced by consideration of the following identity:

$$\left.\frac{ds}{dV}\right|_F=\left(\left.\frac{dh}{dV}\right|_F-\left.\frac{\partial h}{\partial V}\right|_s\right)\left(\left.\frac{\partial h}{\partial s}\right|_V\right)^{-1}$$

$$=\left(\left.\frac{dh}{dV}\right|_F-\left.\frac{\partial h}{\partial V}\right|_s\right)\Big/T\left(1+\frac{\beta a^2}{c_p}\right), \tag{13}$$

which was derived by regarding $h=h(V,s)$, by differentiating along the Fanno line, and then by using (11). As one might expect, a local maximum or minimum in the entropy occurs when the Fanno line is tangent to an isentrope. In the neighborhood of such a tangency point, the relative slopes of the Fanno line and isentropes may be inspected in order to deduce whether the extremum corresponds to a local maximum or minimum in s.

Before giving a more precise criterion which distinguishes between local maxima and minima in the entropy, we first relate the relative slopes of the Fanno lines, and therefore the entropy variation, to the local Mach number. If we combine (10) with the differential of (5), we find that

$$\left.\frac{dh}{dV}\right|_F-\left.\frac{\partial h}{\partial V}\right|_s=\frac{a^2}{V}(1-M^2), \tag{14}$$

where $M\equiv v/a$ is the local Mach number. Thus, tangency points are also sonic points, i.e., points where $M=1$. Furthermore, (13) may now be rewritten

$$\left.\frac{ds}{dV}\right|_F=\frac{a^2}{VT}\frac{1-M^2}{1+\beta a^2/c_p}, \tag{15}$$

from which it is immediately obvious that the entropy increases with an increase in V in subsonic regions and decreases with an increase in V in supersonic regions. This observation is completely consistent with those made in the well-known perfect gas theory.

We now consider the criterion for maxima or minima in the entropy variation along a Fanno line. We note that the slopes of the Fanno line and an isentrope are, by definition, equal at a tangency point so that the nature of the extremum is necessarily determined by the relative curvatures of the Fanno line and the isentrope. If we employ (12) along with the second derivative of (5) and the definition of $\dot{m}$ and M, we can show that

$$\left.\frac{\partial^2 h}{\partial V^2}\right|_s-\left.\frac{d^2 h}{dV^2}\right|_F=\frac{a^2}{V^2}\left(\frac{2\rho\Gamma}{a}+M^2-1\right). \tag{16}$$

Thus, in the neighborhood of the tangency point, denoted by a star, the difference between the enthalpy evaluated on the isentrope, h_s, and that evaluated on the Fanno line, h_F, is

$$h_s-h_F\approx a_*^2\left(\frac{\rho\Gamma}{a}\right)\Big|_*\left(\frac{V-V_*}{V_*}\right)^2+o\left(\frac{V-V_*}{V_*}\right)^2. \tag{17}$$

As a result, we conclude that the isentrope lies above the Fanno line in the neighborhood of a sonic, i.e., tangency, point if $\Gamma>0$ there and it lies below the Fanno line if $\Gamma<0$ at the sonic point. If we employ (11), it is now easily verified that any tangency point corresponds to a local maximum in entropy if and only if $\Gamma>0$ there and is a local minimum if and only if $\Gamma<0$ there. This conclusion relating the nature of the extremum to the fundamental derivative was first given explicitly by Thompson.[16] It is interesting to note that the key connection between Γ and the second derivative of s was also given by Landau and Lifshitz.[14] Our results are summarized in Figs. 3 and 4, where (15) has been employed to determine the Mach number variation.

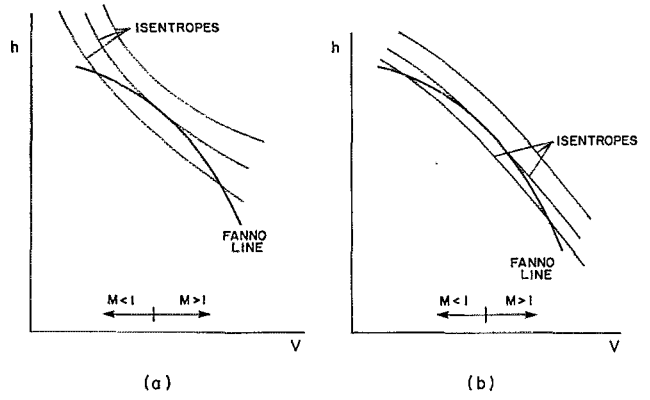

FIG. 3. Sketch of isentropes and Fanno line for (a) $\rho\Gamma/a>\frac{1}{2}$ and (b) $0<\rho\Gamma/a<\frac{1}{2}$ at the tangency, i.e., sonic, point.

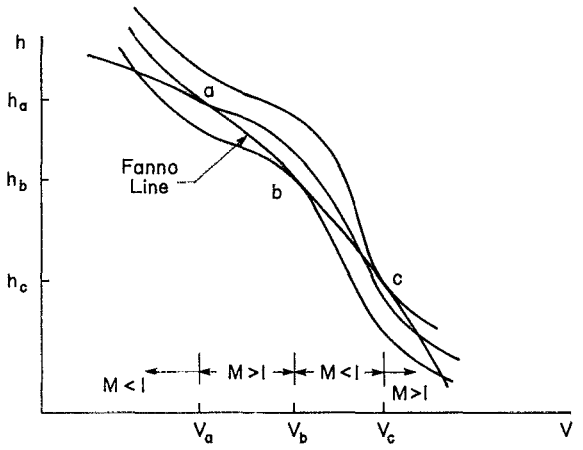

FIG. 5. Sketch of a Fanno line through a $\Gamma<0$ region. Unmarked lines are isentropes. The Fanno line is tangent at points a, b, c.

The majority of the conclusions so far have been concerned with local properties. However, if we consider a fluid for which $\Gamma>0$ at every point in a given Fanno process, then *every* extremum in the entropy necessarily corresponds to a local maximum. Thus, if the process is sufficiently smooth, only one extremum and therefore only one sonic point can exist because of the fact that multiple maxima require the existence of at least one local minima. We therefore conclude that the only Fanno flows for which multiple extrema can exist are those involving BZT fluids. Because the positive Γ flows will, for the most part, turn out to be qualitatively similar to those found in the perfect gas theory, the remainder of the discussion will focus on the behavior of BZT fluids.

A typical Fanno curve and isentropes for a BZT fluid are sketched in Fig. 5. The main assumption in this sketch is that $\Gamma<0$ only over a finite range of volumes V and that a sonic point does occur in the $\Gamma<0$ region. If (11) is employed, it may be shown that

$$s_c>s_a>s_b,$$

where, by definition, $V_c>V_b>V_a$. However, other configurations may be constructed for which $s_a>s_c>s_b$. The corresponding image of the Fanno curve in the s-h plane may now be determined by combining (15) with the derivative of (5) and the definitions of $\dot{m}$ and M to yield

$$\left.\frac{ds}{dh}\right|_F=\frac{1}{TM^2}\frac{M^2-1}{1+\beta a^2/c_p}. \tag{18}$$

Thus the slope of the Fanno line in the s-h plane is positive if the flow is supersonic and it is negative if the flow is subsonic. The Fanno curve corresponding to Fig. 5 has been sketched in Fig. 6. The arrows in the latter figure indicate the flow direction consistent with (7).

The pressure variations required to realize these nonclassical flows can be determined through use of Gibbs' equation (9), the result of which is

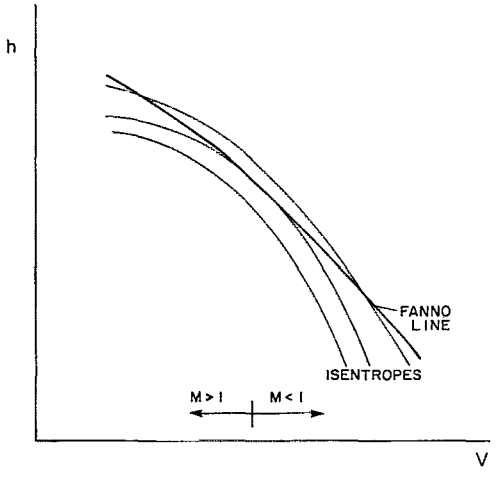

FIG. 4. Sketch of isentropes and Fanno line for $\Gamma<0$ at the tangency, i.e., sonic, point.

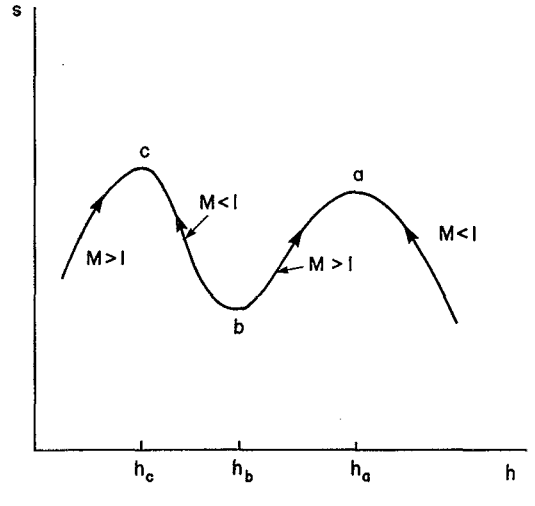

FIG. 6. Sketch of the Mollier (s-h) diagram corresponding to the Fanno line of Fig. 5. Arrows indicate the direction of variation in flow direction.

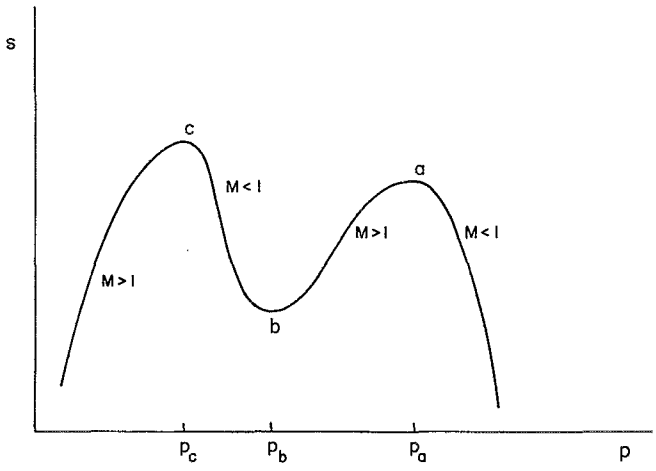

FIG. 7. Sketch of the p-s diagram for the Fanno line of Fig. 5.

$$\left.\frac{dp}{ds}\right|_F = \frac{T}{V}\frac{1+M^2(\beta a^2/c_p)}{M^2-1}. \tag{19}$$

Equation (19) may be shown to be completely equivalent to the result given by Landau and Lifshitz.[14] Thus the pressure increases with s, and therefore the flow direction, in supersonic flows and decreases as s and x increase whenever the flow is subsonic. If (18) and (19) are combined it is easily demonstrated that

$$\left.\frac{dp}{dh}\right|_F = \frac{1}{VM^2}\frac{1+M^2(\beta a^2/c_p)}{1+\beta a^2/c_p} > 0. \tag{20}$$

Thus $p_a > p_b > p_c$ in the case depicted in Figs. 5 and 6. The image of the Fanno line of Figs. 5 and 6 is sketched in Fig. 7 in the p-s plane.

We note that the local behavior suggested by (18)–(20) is exactly the same as that of the perfect gas theory. The main differences between the perfect gas and general fluid behavior is the existence of the local minimum in s and the global structure.

Finally, we consider the Mach number variations on the Fanno line. In particular, we note that the Mach number necessarily attains at least one extremum between the neighboring sonic points seen in Figs. 5–7. Cramer and Best[27] have shown that a fairly simple criterion exists for such extrema provided the flow is isentropic. Because of the entropy variation in Fanno flows, such a simple criterion does not appear possible. The exact expression for the variation of M on the Fanno line can be written

$$\left.\frac{dM}{d\rho}\right|_F = \frac{M}{\rho}\left(-\frac{\rho\Gamma}{a}+\frac{a}{T}\left.\frac{\partial a}{\partial s}\right|_\rho \frac{1-M^2}{1+\beta a^2/c_p}\right). \tag{21}$$

Although

$$\left.\frac{\partial a}{\partial s}\right|_\rho > 0$$

in the ideal gas limit, this derivative can change sign in the dense gas regime, and no simple conclusion regarding the extrema of the M-ρ variation appears possible. However, some insight can be obtained by restricting our attention to near-sonic flows ($M \approx 1$) with $\rho\Gamma/a$ of order one. Under these conditions, (21) may be approximated by

$$\left.\frac{dM}{d\rho}\right|_F \approx -\frac{M}{\rho}\frac{\rho\Gamma}{a}+o(1), \tag{22a}$$

or, upon integration,

$$M \approx 1-\left.\frac{\rho\Gamma}{a}\right|_* \frac{\rho-\rho_*}{\rho_*}+o\left(M-1, \frac{\rho-\rho_*}{\rho_*}\right), \tag{22b}$$

where the * again denotes sonic conditions. We conclude that the Mach number attains an extremum whenever Γ changes sign, at least in the near-sonic limit. A similar approximation was derived by Cramer and Crickenberger[28] in their study of the viscous shock structure. We note that (21) and (22) are completely consistent with the following exact result found in the perfect gas theory ($\Gamma > 0$):

$$\left.\frac{dM}{d\rho}\right|_F = -\frac{M}{\rho}\left(1+\frac{\gamma-1}{2}M^2\right) < 0.$$

III. ANALYTICAL SOLUTIONS FOR VAN DER WAALS GASES

To provide a partial verification of the general results derived in Sec. II, we present exact solutions for Fanno flows of van der Waals gases. The van der Waals equation of state reads

$$p = \frac{RT}{V-b}-\frac{\alpha}{V^2}. \tag{23}$$

Here R is the gas constant, and

$$\alpha = \frac{27}{64}\frac{R^2T_c^2}{p_c} \quad \text{and} \quad b = \frac{RT_c}{8p_c} \tag{24}$$

are material constants correcting the ideal gas relation for the presence of intermolecular forces and excluded volume, respectively. The subscript c denotes properties evaluated at the thermodynamic critical point of the fluid. The specific heat at constant volume c_v is a function of temperature only for van der Waals gases; however, we will assume even this variation is negligible in the flows considered in the present section; i.e., we will take

$$c_v = c_v(T) = \text{const}. \tag{25}$$

Through the use of thermodynamic identities, explicit expressions for the enthalpy, thermodynamic sound speed, and entropy of van der Waals gases may be shown to be

$$h = e_{\text{ref}}+\frac{RT}{\delta}\left(1+\frac{\delta V}{V-b}\right)-\frac{2\alpha}{V}-\frac{RT_{\text{ref}}}{\delta}+\frac{\alpha}{V_{\text{ref}}}, \tag{26}$$

$$a = \left[\left(\frac{V}{V-b}\right)^2 RT(1+\delta)-\frac{2\alpha}{V}\right]^{1/2}, \tag{27}$$

$$s = R\left[\frac{\ln(T/T_{\text{ref}})}{\delta}+\ln\left(\frac{V-b}{V_{\text{ref}}-b}\right)\right]+s_{\text{ref}}, \tag{28}$$

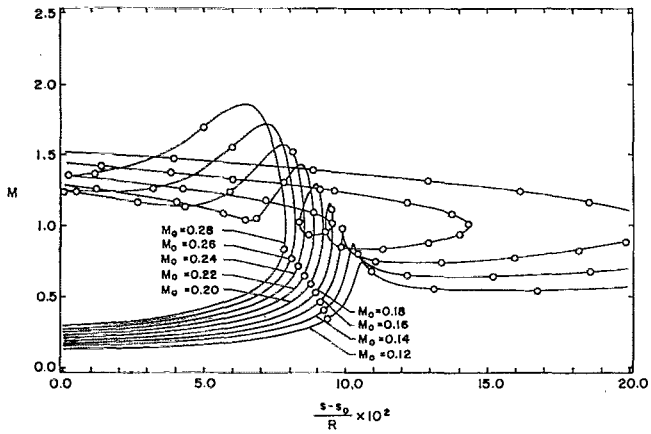

FIG. 8. Computed Mach number variation for a van der Waals gas. The inlet conditions were taken to be $V_0=0.9V_c$, $T_0=1.015T_c$, and the indicated values of M_0. Circles denote the analytical solution of Sec. III and the solid line denotes the numerical solution described in Sec. IV.

where the subscript ref refers to those properties taken to be at an arbitrary reference state, and $\delta=R/c_v$ is a measure of the specific heat.

The temperature variation for a flow of fixed mass flux may now be obtained by combining (26) with (5). After slight rearrangement, we find

$$T=\left[T_0\left(1+\frac{\delta V_0}{V_0-b}\right)+\frac{2\alpha\delta}{RV_0}\left(\frac{V_0}{V}-1\right)+\frac{\delta\dot{m}^2V_0^2}{2R}\left(1-\frac{V^2}{V_0^2}\right)\right]\Big/\left(1+\frac{\delta V}{V-b}\right), \tag{29}$$

where the specific volume and temperature at the pipe inlet are denoted by V_0 and T_0. The mass flux appearing in (29) is found from (4) to be

$$\dot{m}=M_0a_0/V_0, \tag{30}$$

where M_0 and a_0 are the inlet Mach number and sound speed, respectively. The Mach number at any point is obtained by combining the definition $M\equiv v/a$ with (4) to yield

$$M=\dot{m}\frac{V}{a}=M_0\frac{V}{V_0}\frac{a_0}{a}. \tag{31}$$

In the following, we fix the inlet conditions by specifying V_0, T_0, and M_0. The fluid is specified by choosing the critical properties, the molecular weight, and δ. The critical properties and molecular weight were then used to compute the van der Waals parameters (24). The numerical value of the mass flux was computed by combining (27), evaluated at V_0, T_0, and (30). Various values of $V>V_0$ were chosen and substituted in (29). The resultant V, T pairs were then substituted in (26)–(28) and (31) to obtain the flow enthalpy, entropy, and Mach number.

As an example, we have computed and plotted the Mach number and scaled enthalpy versus scaled entropy in Figs. 8 and 9 for the heat transfer and Rankine cycle fluid FC-75 ($C_8H_{16}O$); physical properties were taken from Yarrington and Kay.[29] The initial volume and temperature were taken to be $V_0=0.9V_c$ and $T_0=1.015T_c$. Each curve corresponds to a different inlet Mach number, i.e., mass flux. The actual points computed are denoted by circles, whereas the solid lines correspond to the numerical solution described in the following section. The flows corresponding to $M_0=0.18$ and 0.20 are the nonclassical cases described in Sec. II. The case $M_0=0.16$ is on the boundary between the classical and nonclassical cases. At $M_0=0.18$ and 0.20, the local minimum in the entropy is clearly seen in each of the figures. In Fig. 8, the three sonic points characteristic of nonclassical cases may also be seen. Although no explicit discussion was given in the previous

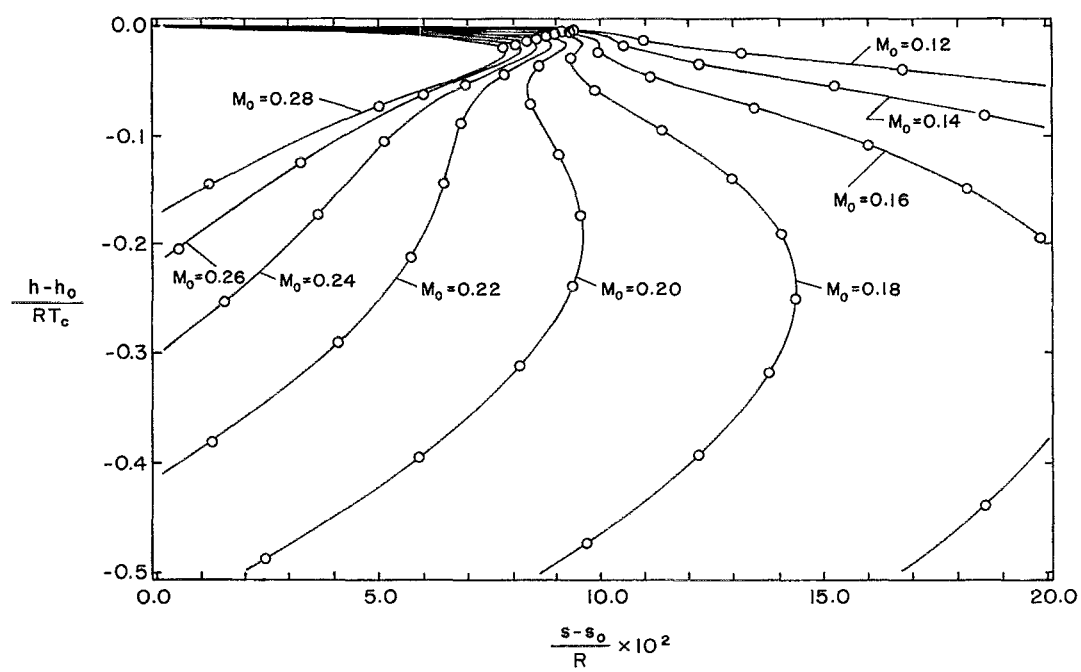

FIG. 9. Computed enthalpy variation for the flows of Fig. 8. The circle and solid lines again denote the analytical and numerical solutions.

section, the M vs s curves are necessarily looped when multiple sonic points occur; this looping phenomenon is also clearly visible in Fig. 8.

IV. NUMERICAL SCHEME

One way to obtain numerical solutions for the Fanno flow is to solve (4) and (5) as an algebraic system. Here we take a different approach in that we consider the differential form of these equations. We should point out that there is no particular advantage of one approach over the other. The choice made here is simply a matter of personal preference.

For a fixed mass flux, we may consider (5) to be the algebraic relation between temperature and specific volume. We may then differentiate (5) with fixed $\dot{m}$ to find

$$\frac{dT}{dV}=\frac{V}{c_v+Vp_T}\left(\frac{a^2}{V^2}\frac{1-\beta T}{\gamma}-\dot{m}^2\right), \tag{32}$$

where γ is the ratio of specific heats and

$$p_T\equiv\left.\frac{\partial p}{\partial T}\right|_V.$$

In any specific case of interest, the gas model will be known, and all thermodynamic parameters appearing in (32) will be known functions of V and T. The constant mass flux $\dot{m}$ can be determined by the inlet conditions. As in the previous section, we take the inlet conditions to be V_0, T_0, and M_0. The approach taken here was to integrate (32) numerically subject to the initial condition $T=T_0$ at $V=V_0$. Because $h(V,T)$, $s(V,T)$, and $a(V,T)$ will also be known once the equation of state is specified, each T,V pair may then be substituted in the above thermodynamic functions to compute the enthalpy, entropy, and sound speed for each $V>V_0$. The Mach number can be computed from an expression similar to (31).

As a check on this computation scheme, we first considered the van der Waals model introduced in Sec. III. The results for the same example used in Sec. III are plotted in Figs. 8 and 9. The numerical scheme is in excellent agreement with the analytical solutions described in Sec. III. Based on this comparison, as well as others involving both perfect gas and van der Waals exact solutions, we conclude that the numerical scheme provides an accurate representation of the exact solutions.

V. COMPUTATIONS USING THE MARTIN–HOU EQUATION

In this section, we present numerical results for the Martin–Hou[21] equation of state. The Martin–Hou equation was chosen for its accuracy, versatility, and widespread use in applications.

The basic form of the equation of state, entropy, internal energy, and specific heat are given in the article by Cramer and Best.[27] Complete details are found in the original article by Martin and Hou.[21] We have also checked our solutions for pressure and temperature against a standard vapor pressure model due to Riedel[30] in order to ensure that the flow remained single phase. If any point in the Fanno process was found to be in the two-phase regime, the whole curve was discarded as invalid.

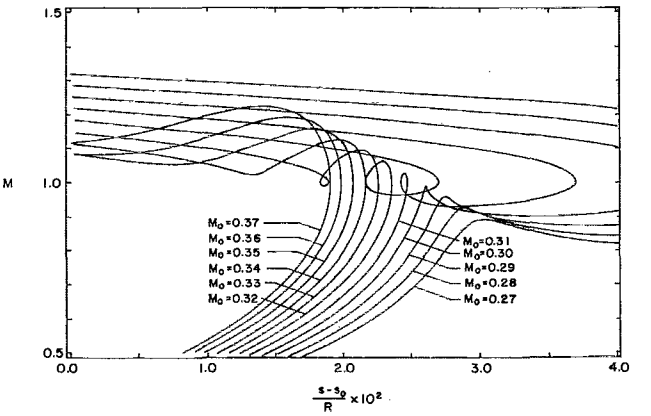

FIG. 10. Computed Mach number variation for PP11 ($C_{14}F_{24}$). The inlet conditions are $V_0=0.75V_c$, $T_0=1.012T_c$, and the indicated values of M_0.

The fluid used is the commercially available heat transfer fluid PP11. As pointed out in the Introduction, the pertinent physical properties are summarized by Cramer.[20]

Results for a range of inlet Mach numbers are plotted in Figs. 10–12. The inlet thermodynamic state was taken to be $V_0=0.75V_c$ and $T_0=1.012T_c$, which corresponds to an inlet pressure and temperature of 16.9 atm and 657.95 °K, respectively. As in the calculations involving van der Waals gases, the characteristic looping of the Mach numbers and multiple extrema in s are observed.

We have also examined the values of $\rho\Gamma/a$ along the Fanno lines depicted in Figs. 10–12. It was found that the extrema in M closely corresponded to the points at which Γ changed sign. This observation is seen to be in complete agreement with the conclusion based on the near-sonic approximation (22).

VI. REMARKS ON SHOCKED FLOWS

In the well-known perfect gas theory of Fanno flows, shock waves can occur if the inlet flow is supersonic. In the case of Fanno flows of BZT fluids, such shocked flows are likely to be considerably more complicated. In order to further emphasize the differences between the behavior of perfect and dense gases, we will simply point out one or two of the most interesting possibilities.

In all that follows, the shock waves will be chosen to satisfy the well-known necessary conditions for an admissible shock. In particular, the entropy inequality will always be satisfied and the shocks will be expected to satisfy the speed-ordering condition

$$M_1>1>M_2, \tag{33}$$

where subscripts 1 and 2 denote conditions immediately upstream and downstream of the shock, respectively. Although other conditions will be discussed, it is important to note that the present discussion should be regarded as entirely conjectural; a more comprehensive and rigorous presentation will be provided at a later date.

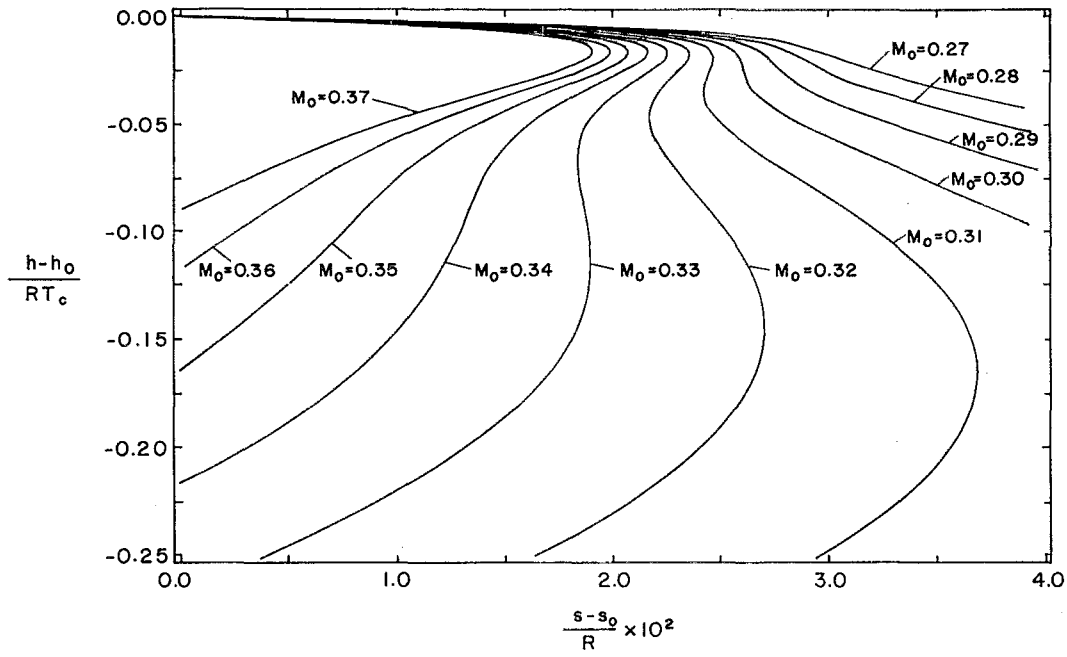

FIG. 11. Computed enthalpy variation for the flow of Fig. 10.

We begin by considering a flow of the type depicted in Figs. 5–7, where the entropy of the high-pressure sonic point is less than that of the low-pressure maxima in entropy. One of the simplest nonclassical cases is the path marked $O'-s_u-A-s_l$ in Fig. 13(a). The pressure distribution corresponding to this flow is sketched in Fig. 13(b). In this case, the sonic ($M_{s_u}=1$) expansion shock s_u-A can be constructed which implies that the flow may be continued up to the lower sonic point s_l. In this example, the main point of interest is that an inspection of the global nature of the Fanno curve of BZT fluids strongly suggests that the flow may be continued even when a sonic point is encountered. A similar continuation beyond sonic points was seen to be possible in the nozzle flows studied by Warner,[31] Chandrasekar and Prasad,[32] Kluwick,[33] and Cramer and Fry.[34] A second point of interest is that a shock is possible even though the inlet flow is subsonic. In the perfect gas theory of Fanno flows, an initially subsonic

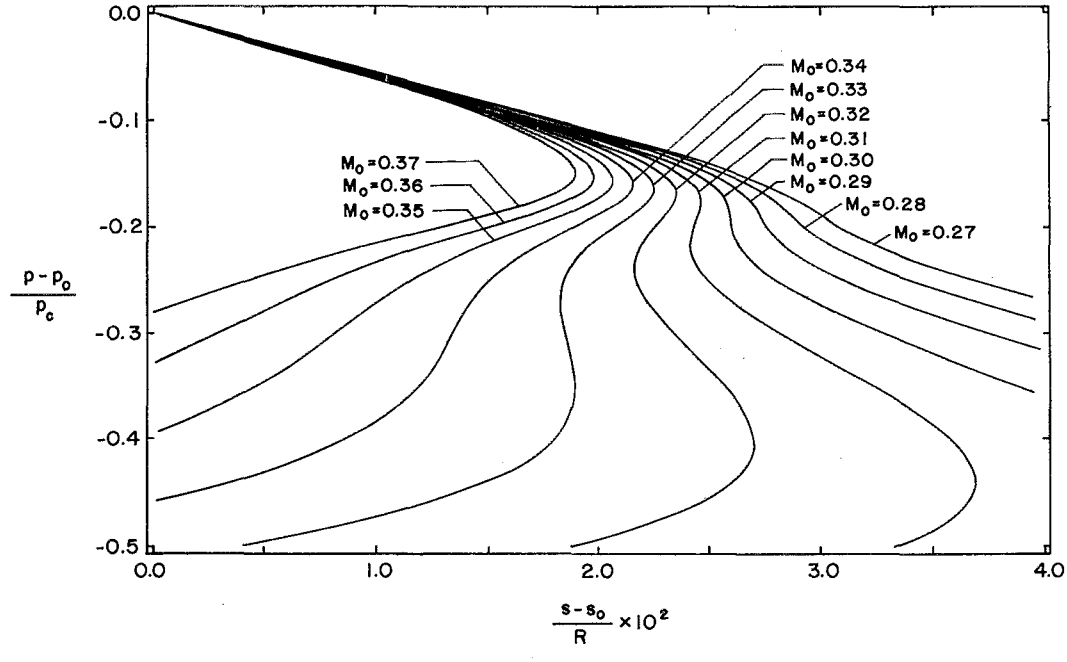

FIG. 12. Computed pressure variation for the flow of Fig. 10.

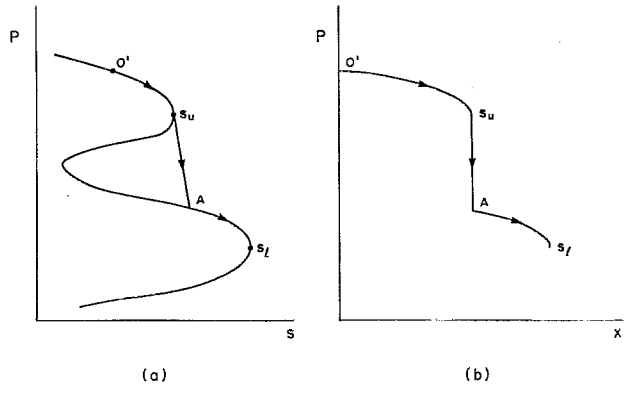

FIG. 13. Sketch of shocked Fanno flow, (a) *p-s* diagram, (b) *p-x* diagram. The subsonic inlet condition is taken to be at *O'*.

flow always remains subsonic and therefore shock free.

The second set of cases involving shocks is illustrated in Fig. 14. The inlet state 0″ is taken to be on the supersonic branch in the general neighborhood of the $\Gamma<0$ sonic point. The first flow follows the path $0''$–A–B–s_u–C–s_l which includes the ordinary compression shock A–B and the sonic expansion shock s_u-C. This path is clearly nonclassical in that two shock waves are involved in a single flow. The second path $0'' - A - C' - s_l'$ involves only a single nonsonic expansion shock A–C'. In Fig. 14(b) we have allowed for the fact that the pipe length corresponding to the sonic condition s_l is likely to be different if different numbers of shocks are present.

In concluding this section, we simply note that the nonclassical shape of the Fanno curves may give rise to shocked flows which differ significantly from those described in the perfect gas theory. Further study is clearly required in order to delineate the full range of possibilities and any limitations.

VII. CONCLUSIONS

The present study has provided a general theory of Fanno flows of single-phase gases. The principal advantage of this work over that of Thompson[16] is that we delineate the global character of the Fanno curve, and are not restricted to flows having Γ strictly positive or strictly negative. The advantage over the well-known perfect gas theory is that the scope is extended to include a far wider range of pressures and temperatures than can be described by the low-pressure theory.

Although only one sonic point corresponding to a local maximum in entropy is expected in flows having $\Gamma>0$, as many as three sonic points corresponding to two maxima and one minimum in s may occur in BZT fluids. A more detailed inspection of the data leading to Figs. 8, 9, 10–12 reveals that the occurrence of $\Gamma<0$ on the Fanno curve is not sufficient to generate the local minimum in the entropy. Once the Fanno curve enters the $\Gamma<0$ region, (22) suggests that the Mach number will attain an extremum and the subsequent Mach number variation will be such that $M\to 1$. The third sonic point will be observed if $M=1$ before the Fanno line passes out of the $\Gamma<0$ region. If, on the other hand, the Fanno curve encounters the $\Gamma=0$ point before the Mach number becomes one, (22) suggests that a local maximum or minimum in M will be attained and the values of M will either decrease or increase away from one, respectively. The resultant *h-s* and *p-s* diagrams will then appear classical.

An important consequence of the local maxima and minima in the Mach number is that it is no longer convenient to use the Mach number to parameterize the Fanno flow. At present, it appears that either the density or specific volume is a better choice. A similar conclusion can be made for isentropic flows.

The nonclassical global structure of the Fanno curves appears to give rise to new configurations for shocked flows. A brief discussion was provided in Sec. VI; a more comprehensive theory will be provided in future publications.

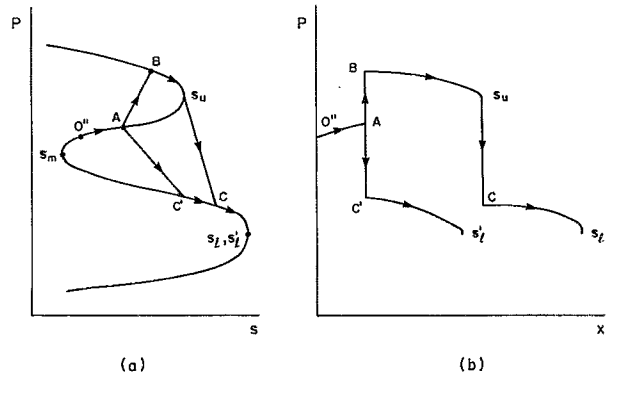

FIG. 14. Sketch of shocked Fanno flows with the supersonic inlet condition *O″*. (a) *p-s* diagram, (b) *p-x* diagram.

ACKNOWLEDGMENTS

This work was supported by the National Science Foundation under Grant No. CTS-8913198.

[1]P. A. Thompson, *Compressible-Fluid Dynamics* (McGraw-Hill, New York, 1972).
[2]J. B. Jones and G. A. Hawkins, *Engineering Thermodynamics*, 2nd Ed. (Wiley, New York, 1986).
[3]F. M. White, *Fluid Mechanics*, 2nd Ed. (McGraw-Hill, New York, 1986).
[4]K. R. Enkenhus and C. Parazzoli, "Dense gas phenomena in a free-piston hypersonic wind tunnel," AIAA J. **8**, 60 (1970).
[5]G. Simeonides, *The Aerodynamic Design of Hypersonic Contoured Axisymmetric Nozzles Including Real Gas Effects*, Von Karman Institute for Fluid Dynamics Technical Memorandum No. 43 (Von Karman Institute, Waterloo, 1987).
[6]G. Simeonides, *The VKI Hypersonic Wind Tunnels and Associated Measurement Techniques*, Von Karman Institute for Fluid Dynamics Technical Memorandum No. 46 (Von Karman Institute, Waterloo, 1990).
[7]W. K. Anderson, "Numerical study of the aerodynamic effects of using sulfur hexafluoride as a test gas in wind tunnels," NASA Technical Paper 3086 (1991).
[8]W. K. Anderson, "Numerical study on using sulfur hexafluoride as a wind tunnel test gas," AIAA J. **29**, 2179 (1991).
[9]J. B. Anders, "Heavy gas wind-tunnel research at Langley Research Center," ASME Paper 93-FE-5.

[10]J. C. Leung and M. Epstein, "A generalized critical flow model for nonideal gases," AIChE J. **34**, 1568 (1988).
[11]W. Bober and W. L. Chow, "Nonideal isentropic gas flow through converging–diverging nozzles," J. Fluids Eng. **112**, 455 (1990).
[12]W. M. Dziedzic, S. C. Jones, D. C. Gould, and D. H. Petley, "Analytical comparison of convective heat transfer correlations in supercritical hydrogen," J. Thermophys. Heat Transfer **7**, 69 (1993).
[13]W. C. Reynolds and H. C. Perkins, *Engineering Thermodynamics*, 2nd Ed. (McGraw-Hill, New York, 1977).
[14]L. D. Landau and E. M. Lifshitz, *Fluid Mechanics* (Addison-Wesley, Boston, 1959).
[15]V. Arp, J. M. Persichetti, and Chen Guo-bang, "The Grüneisen parameter in fluids," J. Fluids Eng. **106**, 193 (1984).
[16]P. A. Thompson, "A fundamental derivative in gas dynamics," Phys. Fluids **14**, 1843 (1971).
[17]H. A. Bethe, "The theory of shock waves for an arbitrary equation of state," Office of Scientific Research and Development, Report No. 545, 1942.
[18]Ya. B. Zel'dovich, "On the possibility of rarefaction shock waves," Zh. Eksp. Teor. **4**, 353 (1946).
[19]R. C. Reid, J. M. Prausnitz, and B. E. Poling, *The Properties of Gases and Liquids*, 4th Ed. (Wiley, New York, 1987).
[20]M. S. Cramer, "Negative nonlinearity in selected fluorocarbons," Phys. Fluids A **1**, 1894 (1989).
[21]J. J. Martin and Y. C. Hou, "Development of an equation of state for gases," AIChE J. **1**, 142 (1955).
[22]K. Lambrakis and P. A. Thompson, "Existence of real fluids with a negative fundamental derivative Γ," Phys. Fluids **15**, 933 (1972).
[23]P. A. Thompson and K. Lambrakis, "Negative shock waves," J. Fluid Mech. **60**, 187 (1973).
[24]R. Menikoff and B. Plohr, "Riemann problem for fluid flow of real materials," Rev. Mod. Phys. **61**, 75 (1989).
[25]P. Leidner, "Realgaseinflusse in der Gasdynamik," Diplomarbeit, Universität Karlsruhe, 1990.
[26]M. S. Cramer, "Nonclassical dynamics of classical gases," in *Nonlinear Waves in Real Fluids*, edited by A. Kluwick (Springer-Verlag, New York, 1991), p. 91.
[27]M. S. Cramer and L. M. Best, "Steady isentropic flows of dense gases," Phys. Fluids A **3**, 219 (1991).
[28]M. S. Cramer and A. B. Crickenberger, "The dissipative structure of shock waves in dense gases," J. Fluid Mech. **223**, 325 (1991).
[29]R. M. Yarrington and W. B. Kay, "Thermodynamic properties of perfluoro-2-butyltetra-hydrofuran," J. Chem. Eng. Data **5**, 24 (1960).
[30]L. Riedel, "Eine neue Universelle Dampfdruckformel-Untersuchungten über eine Erweiterung des Theorems der übereinstimmenden Zustand. Teil 1," Chem. Ing. Tech. **26**, 83 (1954).
[31]S. M. Warner, "Steady non-isentropic flows of dense gases," Virginia Polytechnic Institute and State University, Report No. VPI-E-90-24, 1990.
[32]D. Chandrasekar and Ph. Prasad, "Transonic flow of a fluid with positive and negative nonlinearity through a nozzle," Phys. Fluids A **3**, 427 (1991).
[33]A. Kluwick, "Transonic nozzle flow of dense gases," J. Fluid Mech. **247**, 661 (1993).
[34]M. S. Cramer and R. N. Fry, "Nozzle flows of dense gases," Phys. Fluids A **5**, 1246 (1993).